

Kepler Map for H atom driven by microwaves with arbitrary polarization

PROT PAKOŃSKI

AND

JAKUB ZAKRZEWSKI

Instytut Fizyki im. Mariana Smoluchowskiego, Uniwersytet Jagielloński,
ul. Reymonta 4, 30-059 Kraków, Poland

Dynamics of hydrogen atom driven by microwave field of arbitrary polarization is approximated by the discrete mapping. The map describes the change of dynamical variables from an aphelion or a perihelion to the next one. The results are compared with numerical simulation and previous approximations.

PACS numbers: 05.45.+b, 32.80.Rm

1. Introduction

The microwave ionization of Rydberg atoms, a standard topic in the discussion of the classical–quantum correspondence in classically chaotic systems [1, 2, 3, 4], brings still to us new challenges and surprises. The development of experimental techniques allows one now to vary experimentally the microwave polarization [5, 6]. That in turn enables an efficient control of the dynamics and is a challenging problem for theoretical study [7, 8, 9, 10]. As it becomes now more and more clear, different quantum initial states contribute predominantly to the onset of the ionization when the microwave polarization changes [6, 11].

The full numerical quantal description of the problem becomes within reach of the present days computers. Still simplified models have contributed a lot to our understanding of the mechanism of excitation of an atom and its subsequent ionization especially in term of classical chaos on one side and dynamical localization in the quantum approach [2]. Among such a simplified description a special place is taken by the Kepler map [12, 13, 14, 2] where the full continuous dynamics is approximated by a

discrete mapping. The name Kepler map was introduced in [13]. This map could be used both to classically estimate the experimental ionization threshold as well as to give the quantum mechanical predictions after an appropriate quantization [13, 2, 15, 16].

The main idea behind the mapping approach is an understanding that the electronic motion on the Kepler orbit is the most sensitive to an external microwave perturbation when the electron passes in the vicinity of the nucleus. Such an approach was first applied to a straight line orbit (one-dimensional approximation) [12, 13, 14]. This approach was further developed and quantized by Casati, Guarneri and Shepelyansky [13, 2]. The kicked-like dynamics assumes a Kepler electronic motion between passages at perihelions and the kick every time the electron is at perihelion. One may then obtain the map describing the dynamics between the successive passages at perihelions, or, as proposed in [2], to make the map describing the change of dynamical variables from an aphelion to the next one. To calculate the kick strength the influence of microwaves over whole Kepler period was integrated. This is why the Kepler Map may be seen also as the approximation of the mapping generated by Poincaré section at radial momentum $p = 0$ [17]. This argument shows that approximation should be also valid when the electron orbit stops to be linear. Further approximations [2] lead to a map equivalent to a standard Chirikov map [18]. The quantum mechanical behavior of the latter is well understood [19] leading to an explanation of classical–quantum differences in microwave ionization of H atoms in terms of the Anderson (dynamical) localization.

The authors of [2] extended their analysis to the circular microwave polarization. However, soon Nauenberg showed [17] that the dynamical variables in the derivation of the Kepler Map are not canonically conjugate. He derived the Kepler Map for H atom in circularly polarized microwaves.

We propose the construction of the Kepler Map for H atom subjected in microwaves of arbitrary polarization. This construction allows us to answer questions concerning “canonicity” of variables in previous works. We analyze the limiting cases of the linear motion of the electron in the same linear polarization of the microwave field, and the circular polarization of the microwaves. Our new Kepler Map reduces to the previous approaches in both cases. We compare the map with numerically integrated equations of motion and study validity of the approximation. Further, surprising limitations of such an approach are discussed.

2. Construction – one dimensional model

The Hamiltonian of one dimensional (1D) hydrogen atom in microwave fields reads (in atomic units)

$$H = \frac{p^2}{2} - \frac{1}{x} + Fx \cos \omega t \quad (1)$$

where (x, p) are the position and momentum variable, F is the amplitude of microwaves and ω their frequency. The motion takes place for $x > 0$. Perihelions of the motion described by this Hamiltonian correspond to the point $x = 0$, when the electron bounces from the nucleus. Momentum $p = dx/dt$ then is infinite but the whole Hamiltonian H has finite limit for every $x \rightarrow 0$. To eliminate the time dependence of H we go to an extended phase space [18] with (H, t) being the second pair of variables. The new autonomous Hamiltonian is

$$\mathcal{H} = \frac{p^2}{2} - \frac{1}{x} + Fx \cos \omega t - H = 0, \quad (2)$$

leading to the following equations of motion (ξ is the new time of evolution)

$$\begin{aligned} \frac{dx}{d\xi} &= \frac{\partial \mathcal{H}}{\partial p} = p, & \frac{dp}{d\xi} &= -\frac{\partial \mathcal{H}}{\partial x} = -\frac{1}{x^2} - F \cos \omega t, \\ \frac{dt}{d\xi} &= \frac{\partial \mathcal{H}}{\partial H} = -1, & \frac{dH}{d\xi} &= -\frac{\partial \mathcal{H}}{\partial t} = Fx \omega \sin \omega t. \end{aligned} \quad (3)$$

We evaluate the change of (H, t) variables from a perihelion ($x = 0$) to the next one. These variables are canonically conjugate so the resulting mapping should be a canonical transformation. We introduce the eccentric anomaly u : $\cos u = 1 + 2Ex$. E is the Kepler energy $E = \frac{p^2}{2} - \frac{1}{x}$ of the electron. The parameter u allows us to describe perihelions ($u = 2k\pi$, k integer) and aphelions ($u = \pi + 2k\pi$) of the motion of the electron, since the momentum is equal to $p = \sqrt{-2E \frac{1+\cos u}{1-\cos u}}$. We can calculate $\frac{du}{d\xi}$

$$\frac{du}{d\xi} = \frac{(-2E)^{3/2}}{1 - \cos u} \left(1 + \frac{F}{2E^2} (1 - \cos u) \cos \omega t \right). \quad (4)$$

If $\frac{F}{E^2} < 1$ the derivative $\frac{du}{d\xi}$ may be inverted and the motion of the electron can be parametrized by u

$$\frac{dH}{du} = \frac{F\omega}{(-2E)^{5/2}} \frac{(1 - \cos u)^2 \sin \omega t}{1 + \frac{F}{2E^2} (1 - \cos u) \cos \omega t}, \quad (5)$$

$$\frac{dt}{du} = \frac{-1}{(-2E)^{3/2}} \frac{1 - \cos u}{1 + \frac{F}{2E^2} (1 - \cos u) \cos \omega t}. \quad (6)$$

Integrating these equations to the first order in F/E^2 for $0 \leq u \leq 2\pi$ we obtain 1D Perihelion Kepler Map

$$H' = H + \frac{F\omega}{(-2H')^{5/2}} \int_0^{2\pi} (1 - \cos u)^2 \sin \omega \tau du, \quad (7)$$

$$t' = t - \frac{2\pi}{\omega_K} + \frac{F}{(-2H')^{7/2}} \int_0^{2\pi} [2(1 - \cos u)^2 - 3 \sin u(u - \sin u)] \cos \omega \tau du, \quad (8)$$

where $\tau = (u - \sin u)/\omega_K + t$ is the time obtained from equation (6) integrated in zero order in F/E^2 with $\tau = t$ for $u = 0$ (at perihelion), $\omega_K = (-2H)^{3/2}$ is the Kepler frequency. The condition of area preservation leads to an implicit character of these equations (the right hand side depends on H'). This map is generated by the function G ($H = \frac{\partial G}{\partial t}$, $t' = \frac{\partial G}{\partial H'}$)

$$G(H', t) = H't + \frac{2\pi}{\sqrt{-2H'}} + \frac{F}{(-2H')^{5/2}} \int_0^{2\pi} (1 - \cos u)^2 \cos \omega \tau du. \quad (9)$$

The map (7), (8) coincides with Nauenberg 1D Kepler Map [17], although his map is derived by evaluating the change of Kepler energy E in place of H . For the 1D dynamics the perihelions always take places at $x = 0$, where $E = H$.

The alternative to the perihelion map is the aphelion map. To obtain it we must integrate eqs. (5) and (6) for $-\pi \leq u \leq \pi$ with the new function $\tau = (u - \sin u + \pi)/\omega_K + t$, since now the condition is $\tau = t$ for $u = -\pi$. The 1D Aphelion Kepler Map reads then as follow

$$H' = H + \frac{F\omega}{(-2H')^{5/2}} \int_{-\pi}^{\pi} (1 - \cos u)^2 \sin \omega \tau du, \quad (10)$$

$$t' = t - \frac{2\pi}{\omega_K} + \frac{F}{(-2H')^{7/2}} \int_{-\pi}^{\pi} (1 - \cos u)^2 \left[5 \cos \omega \tau - 3 \frac{\omega}{\omega_K} (u - \sin u + \pi) \sin \omega \tau \right] du. \quad (11)$$

This map does not coincide with Nauenberg 1D Kepler Map [17] any more. Since these equations are related by the condition of area preservation, we can concentrate on the first one (10) only. After integrating by part and some calculation we have

$$H' = H + \frac{F}{-2H'} \sin \left(\omega t + \pi \frac{\omega}{\omega_K} \right) \left[4 \sin \pi \frac{\omega}{\omega_K} - \int_0^{\pi} \sin u \sin \left(\frac{\omega}{\omega_K} (u - \sin u) \right) du \right]. \quad (12)$$

The remaining integral has nice asymptotic behavior for $\omega \gg \omega_K$, this fact serves in [2] to approximate Kepler Map by the standard-like mapping. In the high frequencies regime we find

$$H' = H + F \sin \left(\omega t + \pi \frac{\omega}{\omega_K} \right) \left[\frac{4 \sin \pi \frac{\omega}{\omega_K}}{-2H'} - \frac{2.58}{\omega^{2/3}} \right], \quad (13)$$

$$t' = t - \frac{2\pi}{\omega_K} - F \left[\frac{12\pi}{(-2H')^{7/2}} \cos \left(\omega t + 2\pi \frac{\omega}{\omega_K} \right) + \right. \\ \left. + \frac{7.74\pi}{\omega^{2/3}(-2H')^{5/2}} \sin \left(\omega t + \pi \frac{\omega}{\omega_K} \right) + \frac{8}{\omega(-2H')^2} \cos \left(\omega t + \pi \frac{\omega}{\omega_K} \right) \sin \pi \frac{\omega}{\omega_K} \right]. \quad (14)$$

As in standard map the dependence of H' on t is sinusoidal, but the phase and the amplitude depend on the energy H' . The change of Kepler energy E from a aphelion to the next one is equal to

$$E' = E - \frac{2.58F}{\omega^{2/3}} \sin \left(\omega t + \pi \frac{\omega}{\omega_K} \right), \quad (15)$$

but t is not the canonical conjugate variable to E . Disregarding this fact one could try to perform a canonical change of variables to have new time $T = t + \pi/\omega_K$, keeping the energy E fixed. Then however, to express the mapping in these new variables, first it is necessary to solve an implicit equation, which is an analog to eq. (15).

3. Comparison of one dimensional dynamics

To verify our approximations we have integrated numerically the equations of motion of 1D model of hydrogen atom (3) in parabolic variables. Along each trajectory we have located all aphelions or perihelions. The figure 1 shows the total energies and times (ωt modulo 2π) of subsequent passages by aphelion generated from the numerical integration, 1D Aphelion Kepler Map, and the same map in $\omega \gg \omega_K$ regime. To find the next iteration of the map we solve numerically implicit equations (10) and (13). For $H < -0.6$ the trajectories, found by means of the map, follow ones coming from numerical integration. The approximation breaks down for larger H , because in derivation of the map we have approximated the dynamics only to first order in $\frac{F}{H^2}$. When H approaches to 0 the implicit equation defining the map stops to have unique solution, this fact explains the straight horizontal lines for $H > -0.4$ on the maps picture. Thus while exact dynamics may lead to an unbound diffusion (and subsequently ionization), the map cannot be extended to that regime.

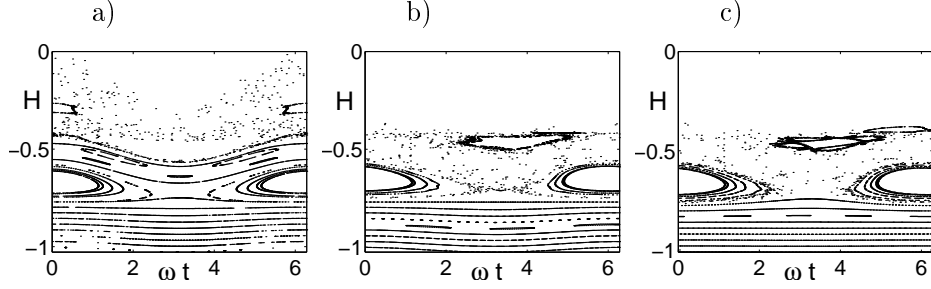


Fig. 1. Comparison of numerically integrated dynamics of 1D hydrogen atom (left panel, denoted as a) with the Aphelion Kepler Map (middle panel, denoted as b) and the same map in the high frequency limit (right panel, c). The total energy H is plotted versus ωt modulo 2π . The amplitude of microwaves $F = 0.02$ and frequency $\omega = 1.6$.

The similar comparison may be performed for the earlier approximations of Kepler dynamics [12, 14, 2]. Figure 2 compares the aphelions found from numerically integrated trajectories, the Kepler Map of Casati et al. [2] and its high frequency limit version. Here the Kepler energy E is plotted

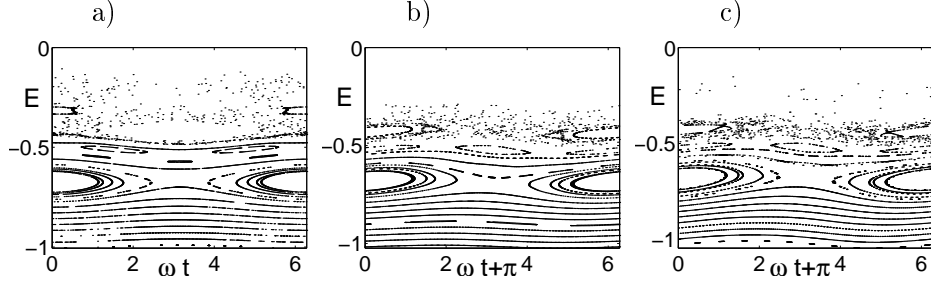


Fig. 2. Comparison of numerically integrated dynamics of 1D hydrogen atom (left panel, denoted as a) with the Kepler Map of Casati et al. [2] (middle panel, denoted as b) and the same map in high frequencies limit (right panel, c). The Kepler energy E is plotted versus ωt modulo 2π , the ωt variable of the map must be shifted by π for correspondence with time. The amplitude of microwaves $F = 0.02$ and frequency $\omega = 1.6$.

versus ωt modulo 2π . The ωt variable for the maps are shifted by π to restore the correspondence with the true time. The use of E as the map variable and the shift of time comes from the definition of the map in [2]. No problem with uniqueness of solutions occurs when iterating these maps

due to asymptotically ($\omega \gg \omega_K$) explicit character of equations defining them.

A similar picture comparing the 1D dynamics with the Kepler Map is shown also for higher frequency $\omega = 3.7$. In figure 3 the trajectories generated from the maps follow the numerically integrated ones for small H . The higher resonances 3:2 and 4:3 ($\omega : \omega_K$) appears stronger and in a different position in the discrete dynamics of the map than in the continuous case. Figure 4 shows that for same frequency $\omega = 3.7$ the canonical transformation of non canonical variable (E, t) may misplace some characteristic part of the phase portrait. The resonance 2:1 is moved by π in the $\omega t + \pi$ variable (the π in the variable comes from the definition of the map).

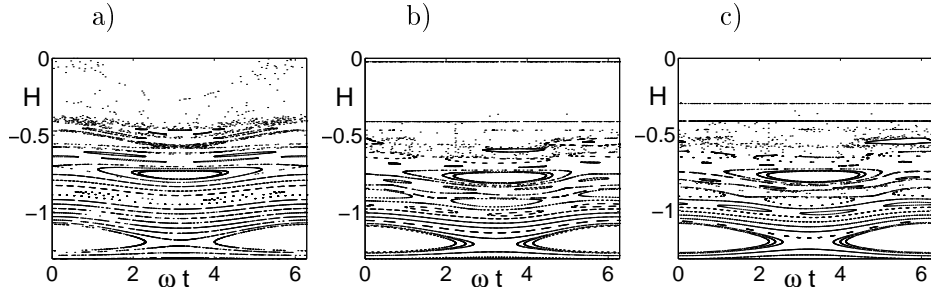


Fig. 3. Same as Fig. 1 but for $F = 0.02$ and $\omega = 3.7$.

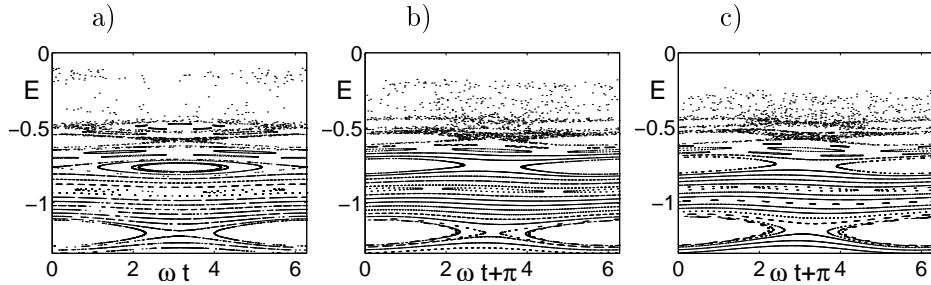


Fig. 4. Same as Fig. 2 but for $F = 0.02$ and $\omega = 3.7$.

We have observed that Perihelion Kepler Map approximates the numerical dynamics of the model for a somewhat larger range of the energies H . The figure 5 shows the Poincaré sections generated from perihelions found from numerically integrated trajectories and found by means of the Kepler Map (as given by the eqs. (7), (8)). The better approximation for larger total energy H may come from the fact, that at perihelions the influence of

perturbation is maximal, the variables change rapidly. The map, obtained by the integration of the influence of the microwaves over the Kepler period, should be better if the interval of integration do not cross the perihelion. Still the map suffers from the same drawback — it is valid locally only, given by implicit equations, which does not have to (and typically do not) yield a unique solution far from the initial conditions. Thus no prediction e.g. for the ionization threshold may be made basing on the “proper”, canonical Kepler map.

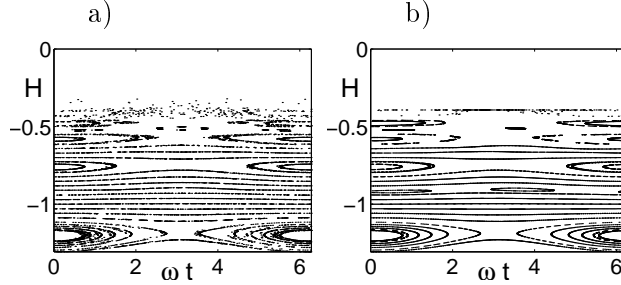


Fig. 5. Comparison of numerically integrated dynamics of 1D hydrogen atom (left panel) with the Perihelion Kepler Map (right). The total energy H is plotted versus ωt modulo 2π . The amplitude of microwaves $F = 0.02$ and frequency $\omega = 3.7$.

4. Construction – two dimensional model

The two dimensional model of hydrogen atom may be perturbed by the microwave field of any polarization. The Hamiltonian of the autonomous system in the extended phase space reads

$$\mathcal{H} = \frac{p^2}{2} + \frac{l^2}{2r^2} - \frac{1}{r} + Fr(\cos \phi \cos \omega t + \alpha \sin \phi \sin \omega t) - H = 0. \quad (16)$$

We use radial coordinate r , ϕ and t as the position variables and p , l , H as the corresponding momenta. The parameter α describes polarization of the microwaves, it ranges from 0 (linear polarization) to 1 (circular one). In analogy to 1D model we introduce the eccentric anomaly defined by $e \cos u = 1 + 2Er$, where E is the Kepler energy $E = \frac{p^2}{2} + \frac{l^2}{2r^2} - \frac{1}{r}$ of the atom and e is the eccentricity $e = \sqrt{1 + 2El^2}$. The points of Poincaré section at $p = 0$ (perihelions and aphelions) are described by $u = k\pi$ with k integer, since

$$p = \sqrt{-2E} \frac{e \sin u}{1 - e \cos u}. \quad (17)$$

If the perturbation is small $F/E^2 \ll 1$, we can find $\frac{dH}{du}$ and $\frac{dl}{du}$ and integrate them for $0 \leq u \leq 2\pi$ to first order in F/E^2

$$H' = H + \frac{F\omega}{(-2H')^{5/2}} \int_0^{2\pi} (1 - e' \cos u)^2 (\cos \theta \sin \omega \tau - \alpha \sin \theta \cos \omega \tau) du, \quad (18)$$

$$l' = l + \frac{F}{(-2H')^{5/2}} \int_0^{2\pi} (1 - e' \cos u)^2 (\sin \theta \cos \omega \tau - \alpha \cos \theta \sin \omega \tau) du, \quad (19)$$

where functions $\tau = (u - e' \sin u)/\omega_K + t$, $\omega_K = (-2H')^{3/2}$ and $\theta = \chi(u) + \phi$,

$$\chi(u) = \int_0^u \frac{\sqrt{1 - e'^2}}{1 - e' \cos u'} du', \quad \sin \chi(u) = \frac{\sqrt{1 - e'^2} \sin u}{1 - e' \cos u}, \quad (20)$$

the eccentricity $e' = \sqrt{1 + 2H'\eta'^2}$. The equations (18) and (19) are generated by the same function

$$G(H', l', t, \phi) = H't + l'\phi + \frac{2\pi}{\sqrt{-2H'}} + 2\pi l' + \frac{F}{(-2H')^{5/2}} \int_0^{2\pi} (1 - e' \cos u)^2 (\cos \theta \cos \omega \tau + \alpha \sin \theta \sin \omega \tau) du. \quad (21)$$

This generating function defines a 2D Perihelion Kepler Map for hydrogen atom perturbed by microwaves of arbitrary polarization¹.

Two limiting cases of the transformation generated by (21) may be verified. The linear motion of the electron along the axis of linearly polarized microwave field corresponds to $l = 0$, $\sin \phi = 0$ and $\alpha = 0$. One can check that the implicit equation (19) for l' has the solution $l' = l = 0$, the $\sin \phi'$ remains 0, because ϕ changes by 2π , and the generating function (21) reduces to the 1D Perihelion Kepler Map (9).

For circularly polarized microwaves $\alpha = 1$ and the integrated function in (21) reduces to $(1 - e' \cos u)^2 \cos(\theta - \omega \tau)$. It depends on t and ϕ via the common variable $\phi - \omega t$. We may canonically change the variables to have $\tilde{\phi} = \phi - \omega t$ and $\tilde{t} = t$, so $\tilde{H} = H + \omega l$ and $\tilde{l} = l$. The generating function of new variables reads as follows

$$G(\tilde{H}', \tilde{l}', \tilde{t}, \tilde{\phi}) = \tilde{H}'\tilde{t} + \tilde{l}'\tilde{\phi} + \frac{2\pi}{\sqrt{-2(\tilde{H}' - \omega\tilde{l}')}} + 2\pi\tilde{l}' + \quad (22)$$

$$\frac{F}{(-2(\tilde{H}' - \omega\tilde{l}'))^{5/2}} \int_0^{2\pi} (1 - e' \cos u)^2 \cos \left(\chi(u) - \frac{\omega}{\omega_K} (u - e \sin u) + \tilde{\phi} \right) du.$$

¹ The very same procedure is possible in 3D where l^2 should be replaced by the total angular momentum squared L^2 .

\tilde{H} is invariant under the transformation (4). It is the autonomous Hamiltonian of the system in the coordinate frame rotating with the microwave frequency. The function (4) generates in variables $(\tilde{l}, \tilde{\phi})$ Nauenberg Kepler Map for circularly polarized microwaves [17].

5. Comparison of two dimensional dynamics

The Poincaré sections generated by 2D Perihelion Kepler Map are four dimensional. The fast dynamics in (H, t) variables is accompanied by the secular motion in (L, ϕ) . Figure 6 shows the (L, ϕ) projection of Poincaré section generated from perihelions found by numerical integration of equations of motion for 2D model of hydrogen atom and found from 2D Perihelion Kepler Map. All trajectories start with $H = -0.5$ and $t = 0$. Small oscillations in trajectories come from the rapid motion in (H, t) variables. The shadow of isolated points placed near $L = 0$ on the Poincaré section

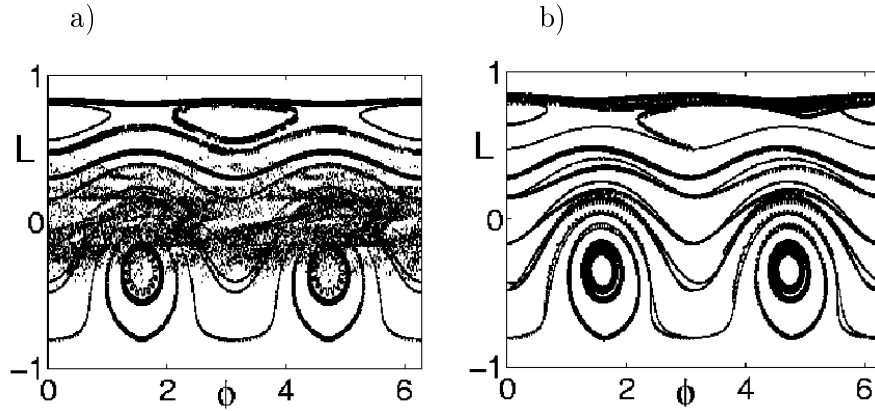


Fig. 6. Comparison of numerically integrated dynamics of 2D hydrogen atom (left panel a) with Perihelion Kepler Map (right panel b). The angular momentum L is plotted versus the radial angle ϕ , this is the projection of Poincaré surface of section so the trajectories may cross. The amplitude of microwaves $F = 0.01$, frequency $\omega = 2$ and the polarization $\alpha = 0.5$.

with numerical trajectories is caused by fact, that the radial angle, at which the perihelion occurs, stops to be well defined for very elongated orbits. The map does not suffer from this problem. To demonstrate this feature we plot (Figure 7) the dependence $L(\phi)$ and $L(t)$ in perihelions for a generic trajectory crossing $L = 0$ with same parameters as in Figure 6. The time dependence of angular momentum shows that the Kepler Map predicts good

values of L at subsequent perihelions. The small error in location of perihelions in the numerically integrated trajectory results in a much bigger error of radial angle, due to a very rapid motion of electron near perihelion, when the orbit is almost linear. The time dependence of the angular momentum L demonstrates that the Kepler Map evolves a little faster than the true dynamics.

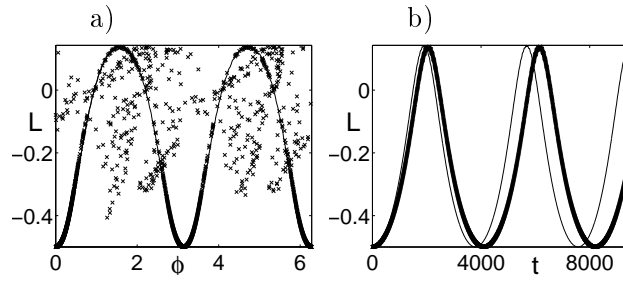


Fig. 7. The dependence of angular momentum L on radial angle ϕ (a) and time t (b) in perihelions for a generic trajectory. The crosses denote ϕ values found from the numerical integration of equations of motion for 2D model of H atom and the solid line is the result of applying 2D Kepler Map. For $L \approx 0$ the radial angle at perihelion is not well defined, this results in isolated points in the left plot. The t dependence does not show a similar problem. The amplitude of microwaves is $F = 0.01$, frequency $\omega = 2$ and the polarization $\alpha = 0.5$.

6. Conclusions

The construction of approximate dynamics of hydrogen atom driven by microwave field of arbitrary polarization by means of a canonical mapping has been presented. The approximation – Kepler Map was compared with numerically integrated dynamics of perturbed H atom and with previously constructed mappings [12, 14, 2]. Although the application of the map requires solving an implicit integral equation, which is not faster than integration of equations of motion, the map may be used to reduce the dimensionality of dynamics and to an approximate quantization.

On the other hand the maps obtained suffer from a major drawback. While being accurate in the vicinity of initial conditions they cease to be so when the electron energy increases significantly due to the diffusion. The effective microwave amplitude becomes then quite strong and the maps, obtained in the first order in F/E^2 , no longer approximate the dynamics. Even worse, they do not yield a unique solutions in that regime. This behavior may be contrasted with the original Kepler map due to Casati and

coworkers [2] which while not canonical and, strictly speaking, incorrect yields some estimate for the onset of chaotic diffusion and ionization. Its other great advantage is the simplicity of its form. Still, it is our opinion, that one should be very cautious while trying to extract any quantitative information from this celebrated mapping due to the shown inconsistencies in its construction.

The support by the Polish Komitet Badań Naukowych under the grant No. 2 P03B 009 18 (P.P.) and 2 P03B 009 15 (J.Z.) is acknowledged.

REFERENCES

- [1] G. Casati *Phys. Rep.* **154**, 77 (1987).
- [2] G. Casati, I. Guarneri, D. L. Shepelyansky, *IEEE J. Quant. Electron.* **24**, 1420 (1988).
- [3] R. V. Jensen *Phys. Rep.* **201**, 1 (1991).
- [4] P. M. Koch, K. A. H. van Leeuwen, *Phys. Rep.* **255**, 289 (1995).
- [5] P. Fu, T. J. Scholz, J. M. Hettema, T. F. Gallagher, *Phys. Rev. Lett.* **64**, 511 (1990).
- [6] M. R. W. Bellerma, P. M. Koch, D. R. Mariani, D. Richards, *Phys. Rev. Lett.* **76**, 892 (1996), *ibid.* **78**, 3840 (1997).
- [7] D. Richards, *J. Phys. B* **25**, 1347 (1992).
- [8] D. Richards, *J. Phys. B* **30**, 4019 (1997).
- [9] E. Oks, T. Uzer, *J. Phys. B* **33**, L533 (2000).
- [10] E. Oks, J. E. Davis, T. Uzer, *J. Phys. B* **33**, 207 (2000).
- [11] K. Sacha, J. Zakrzewski *Phys. Rev. A* **58**, 488 (1998).
- [12] T. Y. Petrosky, *Phys. Lett. A* **117**, 328 (1986).
- [13] G. Casati, I. Guarneri, D. L. Shepelyansky, *Phys. Rev. A* **36**, 3501 (1987).
- [14] V. Gontis, B. Kaulakys, *J. Phys. B* **20**, 5051 (1987).
- [15] B. Kaulakys, G. Vitulis, *Physica Scripta* **59** (4), 251 (1999).
- [16] G. Benenti, G. Casati, G. Maspero, D. L. Shepelyansky *Phys. Rev. Lett.* **84**, 4088 (2000).
- [17] M. Nauenberg, *Europhys. Lett.* **13**, 611 (1990).
- [18] A. J. Lichtenberg, M. A. Lieberman, *Regular and Stochastic Motion*, Springer-Verlag, New York 1983.
- [19] S. Fishman, D. R. Grempel, R. E. Prange *Phys. Rev. Lett.* **49**, 509 (1982), *Phys. Rev. A* **29**, 1639 (1984).